

Experimental and Modeling Study on a Packed-Bed Membrane Reactor for Partial Oxidation of Methane to Formaldehyde

Chao Yang, Nanping Xu,* and Jun Shi

Membrane Science & Technology Research Center, Nanjing University of Chemical Technology, Nanjing 210009, People's Republic of China

A conventional fixed-bed reactor and a hybrid packed-bed membrane reactor are used to investigate the selective oxidation of methane to formaldehyde over a Mo–Co–B–O/SiO₂ catalyst at atmospheric pressure and in the reaction temperature range of 883–963 K. The reaction kinetic rate expressions have been determined by simulating the measured relationships of conversions and selectivities in the fixed-bed reactor. A zirconia/ α -alumina porous membrane packed with the Mo–Co–B–O/SiO₂ catalyst is used as a distributor of reactants in the hybrid membrane reactor. A theoretical model solved by the numerical method of orthogonal collocation has also been developed for the membrane reactors to simulate the experimental data. The effects of reaction process operation conditions and membrane pore sizes on the performance of the inert membrane reactor are examined. The prospects of commercial applications for methane partial oxidations are also discussed.

Introduction

Natural gas, the predominant component of which is methane, is a highly abundant and low-cost carbon source. Although progress toward obtaining a yield that would make a process industrially viable has been very low, the study on the partial oxidation of methane to C₁ oxygenates, such as formaldehyde and methanol, over heterogeneous catalysts at atmospheric pressure has gained increasing attention in recent years as an alternative to the costly, energy-intensive steam-reforming method of production in the current chemical industry.

Several reviews (Fox, 1993; Krylov, 1993; Pitchai and Klier, 1986) have been published about the selective oxidation of methane to formaldehyde and methanol. Many catalysts, mainly including molybdenum oxide-based, metal, zeolite, and other oxide catalysts, have been examined. Among them, catalysts based on silica-supported molybdenum oxide were the most widely studied (Bañares et al., 1994; Lu et al., 1996; Parmaliana et al., 1995; Spencer et al., 1990; Spencer and Pereira, 1987; Spencer, 1988). High selectivities to formaldehyde and methanol at low methane conversion have been reported, but the selectivities drop drastically at increasing conversion, which leads to few studies of yields higher than about 2%. These limited yields arise from the unfavorable reactivity of methane to formaldehyde and methanol, i.e., inert chemical properties of methane and the easy deep oxidation of formaldehyde and methanol.

Up to now, the mechanism over MoO₃-based catalysts is not completely understood. The results achieved by the different research groups, either in terms of selectivity or yield to formaldehyde, are not completely agreeable, and even appear to be controversial. Spencer and co-workers (Bañares et al., 1994; Spencer et al., 1990; Spencer and Pereira, 1987; Spencer, 1988) have

investigated the selective oxidation of methane over redox-type MoO₃ catalysts. The redox mechanism over MoO₃/SiO₂ involves the parallel conversion of methane to HCHO and CO₂, with HCHO being further oxidized to CO. Lu et al. (1996) have evaluated direct oxidation of methane to methanol over Mo–Co–O/SiO₂ catalyst. The maximum yield of methanol obtained is about 0.1%.

Membrane reactors combine two distinctly different functions, i.e., reaction and separation, into a single operation. During the past decade there has been intensified activity in the research and development of porous or dense inorganic membranes for catalytic membrane reactors. Processes utilizing catalytic membrane reactors have the potential for dramatically increasing the yield of reactions that are currently limited by thermodynamic equilibrium, product inhibition, or kinetic selectivity. Examples of commercial interest include hydrogenation, dehydrogenation, partial and selective oxidation, hydrocarbon cracking, hydroformylation, olefin polymerization, etc. A large portion of the most significant reactions falls into the category of high-temperature, gas-phase chemical and petrochemical processes. The studies on inorganic membrane reactors have been well-reviewed (Armor, 1989; Bhave, 1991; Eng and Stoukides, 1991; Sanchez and Tsotsis, 1996; Saracco and Specchia, 1994; Shu et al., 1991). Most of the applications of inorganic membrane reactors proposed to date make use of the permselectivity of membranes, such as palladium alloy membranes for dehydrogenation reactions and perovskite dense membrane reactors for partial oxidation reactions. Another important field of application for membrane reactors involves their use as distributors of reactants. In this case, the porous membranes are used to distribute one or more reactants. This has prompted research for series or parallel oxidation reactions with valuable intermediate products. The selectivities toward the desired products are favored if low oxygen concentrations are controlled (Bhave, 1991; Sanchez and Tsotsis, 1996).

The modeling and simulation of catalytic membrane reactors have also attracted the interest of many

* To whom correspondence should be addressed. Telephone: +86-25-3316755-3099. Fax: +86-25-3300345. E-mail: mst@dns.njuct.edu.cn.

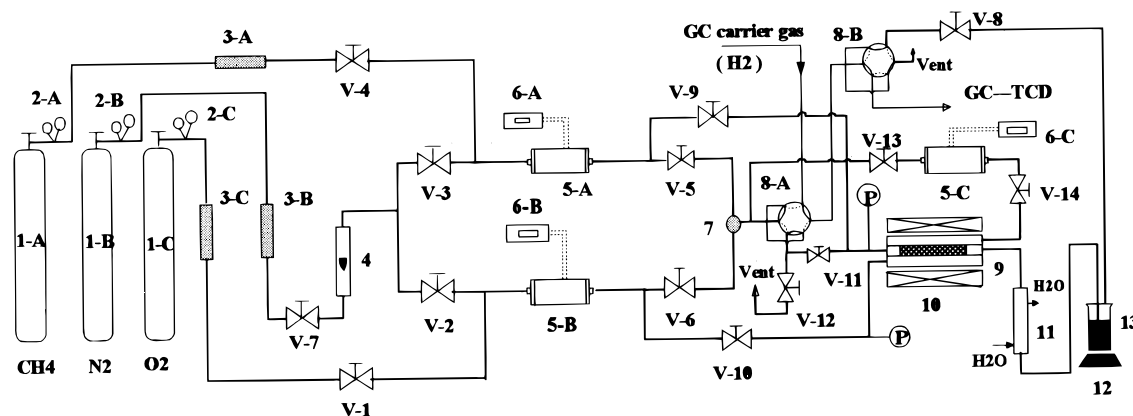


Figure 1. Schematic of the apparatus for fixed-bed and membrane reactions. 1-A,B,C: gas cylinders. 2-A,B,C: gas regulators. 3-A,B,C: purifying traps. 4: rotameter. 5-A,B,C: mass flow sensor-control modules. 6-A,B,C: mass flow controller and digital readouts. 7: gas mixer. 8-A,B: six-way valves. 9: reactor. 10: furnace. 11: cooler. 12: electromagnetic stirrer. 13: absorber. P: pressure gauge. V-1–14: flow control valves.

investigators (Hsieh, 1996; Sanchez and Tsotsis, 1996). Most studies have focused on particular membrane reactor systems aiming to simulate their performance in terms of attainable yield and selectivities. Dehydrogenation of cyclohexane to produce benzene has been studied extensively (Itoh et al., 1988; 1990; Sun and Khang, 1990). Slood et al. (1990, 1992) have modeled the behavior of nonpermeable catalytic membrane reactors using the dusty-gas model description of transport. The membrane reactor utilizing multilayered membranes has been modeled by Becker et al. (1993). The reaction was ethylbenzene dehydrogenation in their isothermal model that accounts for mass transport both through the mesoporous permselective layer and the underlying macroporous support layer. Bindjouli et al. (1994) have developed a similar packed-bed membrane reactor model for alkane dehydrogenation. The models for the operation of three-phase catalytic membrane reactors have also been discussed (Torres et al., 1994). Shu et al. (1994) modeled the data in their studies of methane steam reforming in a catalytic membrane reactor using a Pd–Ag membrane deposited on porous stainless steel. Moreover, there are a number of modeling studies of the application of solid oxide dense membrane reactors for partial oxidation of methane to synthesis gas and methane oxidation coupling (Dixon et al., 1994; Lu et al., 1994; Nozaki and Fujimoto, 1994; Tsai, 1996; Wang and Lin, 1994).

To discover the more commercially feasible route for methane utilization, the partial oxidations of methane to formaldehyde over the silica-supported molybdenum oxide catalysts doped with cobalt and boron in a fixed-bed reactor and a hybrid packed-bed zirconia/ α -alumina membrane reactor are studied in this work. An isothermal membrane reactor model, which takes into account chemical kinetics obtained from the fixed-bed reactor experiment, mass transport through the membrane, and flow pattern in the reactive and separation sides, has also been developed to simulate the experimental data and investigate the feasibility of a membrane reactor for the direct conversion method.

Experimental Section

Catalyst. The silica-supported molybdenum oxide, cobalt oxide, and boron oxide species were prepared by the incipient-wetness impregnation method with an

aqueous solution of ammonium heptamolybdate ($(\text{NH}_4)_6\text{Mo}_7\text{O}_{24}\cdot 4\text{H}_2\text{O}$), cobaltous nitrate ($\text{Co}(\text{NO}_3)_2\cdot 6\text{H}_2\text{O}$), and boric acid (H_3BO_3), respectively. The pH values of the impregnating solutions were adjusted with nitric acid or ammonia liquor. The particle size fraction of the silica used (with BET specific surface area of $248\text{ m}^2/\text{g}$, by Sorptomatic 1900) is 40–70 mesh. After each process of impregnation, the samples were dried overnight under ambient conditions and dried at 393 K for 4 h. Then the dry samples were calcined at 873 K for 8 h in a temperature-programmable furnace. The obtained catalyst contains 5 wt % MoO_3 and 5 wt % B_2O_3 . The atomic ratio of Mo/Co is about 5.

Apparatus. The catalytic reactions were carried out in a fixed-bed reactor and a packed-bed membrane reactor under continuous flow of the reaction mixture at atmospheric pressure, using oxygen as the oxidant; the CH_4/O_2 molar ratio was about 7.5/1. The process flow schematic is shown in Figure 1. The experimental system consists of a reactant gas delivery and measurement system, a high-temperature fixed-bed reactor or membrane reactor, and product collection and measurement devices.

A 2-mL sample of catalyst was loaded into the fixed-bed reactor consisting of a dense α -alumina tube within a stainless tube. In the membrane reactor, the catalyst was packed into a homemade zirconia/ α -alumina asymmetric membrane (Huang, 1996) with a mean pore diameter of $0.17\ \mu\text{m}$. The same catalyst bed dimensions and linear gas velocities through the bed were set in fixed-bed and packed-bed membrane reactors. The ceramic membrane tube was sealed in the stainless steel reactor module using graphite gaskets. The catalyst was covered with a certain amount of quartz chips, which formed a preheating zone. The reaction temperature was monitored by a type-K thermocouple placed in contact with the catalyst bed. Another type-K thermocouple was used to control the temperature. A precision programmable temperature controller (YCC-1261, Xiamen Jiuyu Electronic Instrument Allied Co., China) was used to set the temperature parameters.

Analytical Method. Reaction feed streams were maintained at the desired composition and flow rate by flowing methane and oxygen through mass flow controllers (LRZ-3, Shanghai Guanghua Instrument & Meter Plant, China) previously calibrated for each specific gas in this work. The effluent gas was condensed rapidly

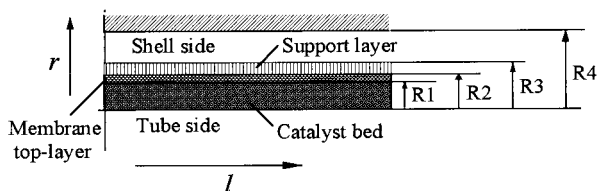


Figure 2. Schematic diagram of the membrane reactor.

with water close to the reactor exit, to prevent the C_1 oxygenates from further oxidizing, and then the liquid product was absorbed in a water absorber maintained at 0 °C by an ice–water mixture. The gaseous feeds and products were analyzed using an on-line gas chromatograph (Shimadzu GC-7A) equipped with two columns in series: (i) a 2 m × 3 mm TDX-01 (Tianjing Chemical Reagent 2nd Plant, China) kept at 100 °C, (ii) 1 m × 3 mm 5A molecular sieve (Shimadzu) kept at 30 °C, which were connected to a thermal conductivity detector (TCD). Hydrogen was used as the carrier gas for gas analysis. Formaldehyde and methanol were cumulatively determined by the same gas chromatograph at the end of each run on the absorbed aqueous solution by a 3 m × 3 mm GDX-403 column (Tianjing Chemical Reagent 2nd Plant, China) kept at 120 °C and connected to a flame ionization detector (FID) with the carrier gas of nitrogen. Calibrations for formaldehyde were obtained with distilled formaldehyde aqueous solutions (stabilized with 8–12% methanol) of different compositions, which were previously analyzed by titration using sodium sulfite (Na_2SO_3) and a sulfuric acid (H_2SO_4) standard aqueous solution.

Theoretical Model

A mathematical model has been developed to simulate the performance of the hybrid packed-bed membrane reactor. This model attempts to describe a general flow pattern in both tube and shell sides through the incorporation of dispersion coefficients. A schematic of the cross section of the membrane reactor is shown in Figure 2. The zirconia/ α -alumina membrane is modeled as a two-layer membrane consisting of one zirconia top layer and a thick α -alumina support layer. The catalyst used is packed in the tube side, but the shell side is empty. The catalytic reaction is operated at a low-pressure (atmospheric pressure) and high-temperature (higher than 873 K) environment. The theoretical model is based on the following assumptions:

- (1) The reactor is at steady state.
- (2) The catalyst particles, the membrane, and the surrounding gas phase are all under isothermal conditions.
- (3) The difference of total pressure between the tube side and the shell side is assumed to be zero. Pressure drops in both the tube and shell regions are also negligible. Radial convective flow is negligible compared to axial flow velocity.
- (4) The membrane pores are of cylindrical shape.
- (5) The homogeneous gas-phase oxidation reactions are negligible.

According to the principles of mass conservation, the design model equations for the hybrid membrane reactor are derived in each of the four regions as given below.

In the tube side, i.e., the catalytic layer: $0 < r < R_1$

$$\epsilon_1 D_{1i} \left(\frac{\partial^2 C_{1i}}{\partial r^2} + \frac{1}{r} \frac{\partial C_{1i}}{\partial r} \right) - u_1 \frac{\partial C_{1i}}{\partial l} - \sum_{n=1}^N \alpha_{ni} \text{RK}_n = 0 \quad (1)$$

where RK_n is the kinetic rate expression of the reaction numbered n .

In the zirconia top-layer: $R_1 < r < R_2$

$$\frac{\partial}{\partial r} \left(r \frac{\partial C_{2i}}{\partial r} \right) = 0 \quad (2)$$

In the support layer: $R_2 < r < R_3$

$$\frac{\partial}{\partial r} \left(r \frac{\partial C_{3i}}{\partial r} \right) = 0 \quad (3)$$

In the shell side: $R_3 < r < R_4$

$$D_{4i} \left(\frac{\partial^2 C_{4i}}{\partial r^2} + \frac{1}{r} \frac{\partial C_{4i}}{\partial r} \right) - u_4 \frac{\partial C_{4i}}{\partial l} = 0 \quad (4)$$

The initial conditions for the different regions are

$$l = 0, \quad C_{ji} = C_{ji}^0$$

where the subscript i is the reaction gas species, CH_4 , O_2 , CO , HCHO , CO_2 , H_2O . $j = 1-4$, i.e., the different regions of membrane reactor, respectively.

The set of equations used to model the four regions are coupled together by their boundary conditions as follows:

At the axis of symmetry in the tube side:

$$r = 0$$

$$\frac{\partial C_{1i}}{\partial r} = 0 \quad (5)$$

At the catalytic layer/zirconia membrane top layer interface:

$$r = R_1$$

$$D_{1i} \frac{\partial C_{1i}}{\partial r} = D_{2i} \frac{\partial C_{2i}}{\partial r}, \quad C_{1i} = C_{2i} \quad (6)$$

At the zirconia top layer/support layer interface:

$$r = R_2$$

$$D_{2i} \frac{\partial C_{2i}}{\partial r} = D_{3i} \frac{\partial C_{3i}}{\partial r}, \quad C_{2i} = C_{3i} \quad (7)$$

At the support layer/shell side interface:

$$r = R_3$$

$$D_{3i} \frac{\partial C_{3i}}{\partial r} = D_{4i} \frac{\partial C_{4i}}{\partial r}, \quad C_{3i} = C_{4i} \quad (8)$$

On the wall of the stainless steel reactor housing:

$$r = R_4$$

$$D_{4i} \frac{\partial C_{4i}}{\partial r} = 0 \quad (9)$$

Equations 2 and 3 can be solved analytically.

$$C_{2i} = \frac{C_{1i} \ln(R_2/r) + C_{3i} \ln(r/R_1)}{\ln(R_2/R_1)} \quad (10)$$

$$C_{3i} = \frac{C_{2i} \ln(R_3/r) + C_{4i} \ln(r/R_2)}{\ln(R_3/R_2)} \quad (11)$$

Dimensionless quantities are defined as

$$0 \leq r \leq R_1, \quad \tilde{r} = \frac{r}{R_1}$$

$$R_1 \leq r \leq R_2, \quad \tilde{r} = \frac{r - R_1}{R_2 - R_1}$$

$$R_2 \leq r \leq R_3, \quad \tilde{r} = \frac{r - R_2}{R_3 - R_2}$$

$$R_3 \leq r \leq R_4, \quad \tilde{r} = \frac{r - R_3}{R_4 - R_3}$$

$$\tilde{C}_{ji} = C_{ji}/C_{CH_4}^0$$

$$\tilde{l} = l/L$$

Then the dimensionless forms of partial differential equations are listed as follows:

In the tube side: $0 < r < R_1$, i.e., $0 < \tilde{r} < 1$

$$\tilde{D}_{1i} \left(\frac{\partial^2 \tilde{C}_{1i}}{\partial \tilde{r}^2} + \frac{1}{\tilde{r}} \frac{\partial \tilde{C}_{1i}}{\partial \tilde{r}} \right) - \frac{\partial \tilde{C}_{1i}}{\partial \tilde{l}} - \sum_{n=1}^N \tilde{\alpha}_{ni} \text{RK}_n^* = 0 \quad (12)$$

in which RK_n^* is the dimensionless form of the kinetic rate expression, and

$$\tilde{D}_{1i} = \frac{\epsilon_1 D_{1i} L}{u_1 R_1^2} \quad \text{and} \quad \tilde{\alpha}_{ni} = \frac{L}{u_1} \alpha_{ni}$$

In the shell side: $R_3 < r < R_4$, i.e., $0 < \tilde{r} < 1$

$$\tilde{D}_{4i} \left(\frac{\partial^2 \tilde{C}_{4i}}{\partial \tilde{r}^2} + \frac{1}{\tilde{r} + R_3/\delta_4} \frac{\partial \tilde{C}_{4i}}{\partial \tilde{r}} \right) - \frac{\partial \tilde{C}_{4i}}{\partial \tilde{l}} = 0 \quad (13)$$

in which

$$\tilde{D}_{4i} = \frac{D_{4i} L}{u_4 \delta_4^2} \quad \text{and} \quad \delta_4 = R_4 - R_3$$

Furthermore, the expressions of $\partial C_{1i}/\partial \tilde{r}$ near $r = R_1$, $\partial C_{2i}/\partial \tilde{r}$ and $\partial C_{3i}/\partial \tilde{r}$ near $r = R_2$, and $\partial C_{4i}/\partial \tilde{r}$ near $r = R_3$ can be obtained by using the C_{2i} and C_{3i} expressions of (10) and (11) together with the boundary conditions of eqs 6–8. Then the dimensionless forms of the boundary conditions satisfying the continuity of the concentrations at both sides of the membrane are derived as the following:

At the catalytic layer/membrane top layer interface:

$$r = R_1, \text{ i.e., } \tilde{r} = 1$$

$$\frac{\partial \tilde{C}_{1i}}{\partial \tilde{r}} = Ak_{1i}(\tilde{C}_{1i} - \tilde{C}_{4i}) \quad (14)$$

At the support layer/shell side interface:

$$r = R_3, \text{ i.e., } \tilde{r} = 0$$

$$\frac{\partial \tilde{C}_{4i}}{\partial \tilde{r}} = Ak_{4i}(\tilde{C}_{1i} - \tilde{C}_{4i}) \quad (15)$$

where

$$Ak_{1i} = - \frac{D_{2i} D_{3i}}{D_{1i}} \frac{1}{R_1} \frac{\delta_1 \delta_3}{D_3 \delta_0 \delta_3 + D_{2i} \delta_1 \delta_2}$$

$$Ak_{4i} = - \frac{D_{2i} D_{3i}}{D_{4i}} \frac{1}{R_3} \frac{\delta_1 \delta_3}{D_3 \delta_0 \delta_3 + D_{2i} \delta_1 \delta_2}$$

and

$$\delta_0 = \ln(R_2/R_1), \quad \delta_1 = R_2 - R_1$$

$$\delta_2 = \ln(R_3/R_1), \quad \delta_3 = R_3 - R_2$$

The above two-dimensional partial differential equations are solved using the numerical method of orthogonal collocation.

Results and Discussion

Fixed-Bed Reactor Experimental and Kinetics Studies. Under the conditions of the present work, the selective oxidation of methane on the Mo-Co-B-O/SiO₂ catalyst yielded essentially HCHO, CO, CO₂, and H₂O; minor amounts of CH₃OH were observed. The yield of methanol, which was neglected in the calculations of product distribution, was consistently below 0.001%.

The influence of the reaction temperature on methane conversion is shown in Figure 3 (space velocity, 4800 h⁻¹; reactants, CH₄/O₂ = 7.5/1; atmospheric pressure). At lower conversion levels, the methane conversion increased slowly with increasing reaction temperature. The conversion increased more rapidly at higher temperature mainly due to the serious deep oxidation. Figure 4 depicts the conversion of methane versus reaction space velocity at two representative reaction temperatures. The increase of space velocity by increasing the feed flowing rate led to a decrease of the contact time of the reaction mixture and catalyst.

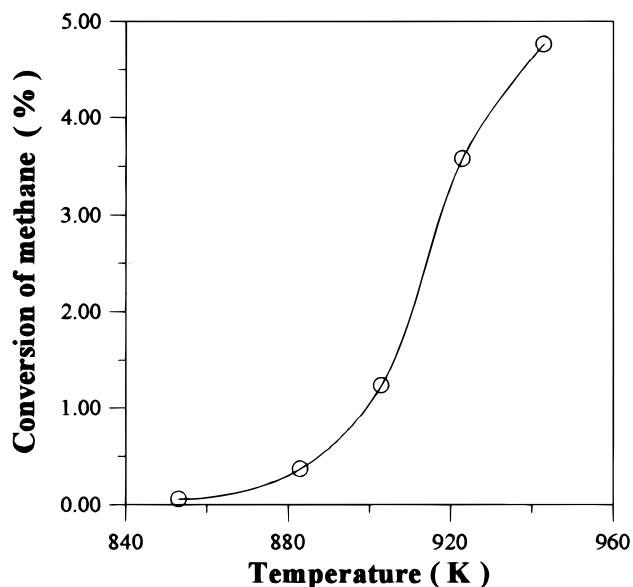


Figure 3. Influence of temperature on methane conversion in a fixed-bed reactor.

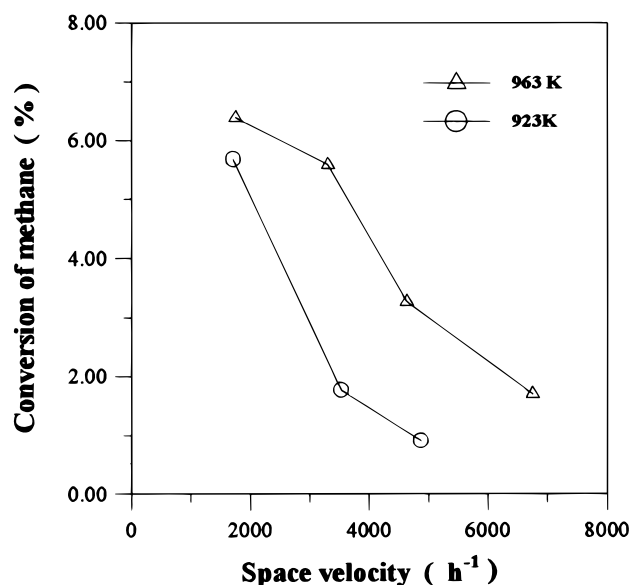


Figure 4. Influence of space velocity on methane conversion in a fixed-bed reactor.

Clearly, the higher space velocity would cause the lower methane conversion.

The selectivity to HCHO, CO, and CO₂ versus methane conversion at different reaction temperatures on the Mo-Co-B-O/SiO₂ catalyst is presented in Figures 5–7 respectively (space velocity, 1000–7000 h⁻¹; reactants, CH₄/O₂ = 7.5/1; atmospheric pressure). Figure 5 demonstrates that the formaldehyde selectivity decreased monotonically with increasing methane conversion. As shown in Figure 6, the selectivity to carbon monoxide increased with methane conversion. The CO selectivity tended to zero at zero methane conversion and became relatively constant at high conversion levels. At high methane conversion, carbon monoxide became the dominant oxidation product. The selectivity to carbon dioxide was very low and did not appear to change very significantly as methane conversion increased (Figure 7). On the basis of the above observations, formaldehyde and carbon dioxide should be the primary catalytic oxidation reaction products, but carbon monoxide was

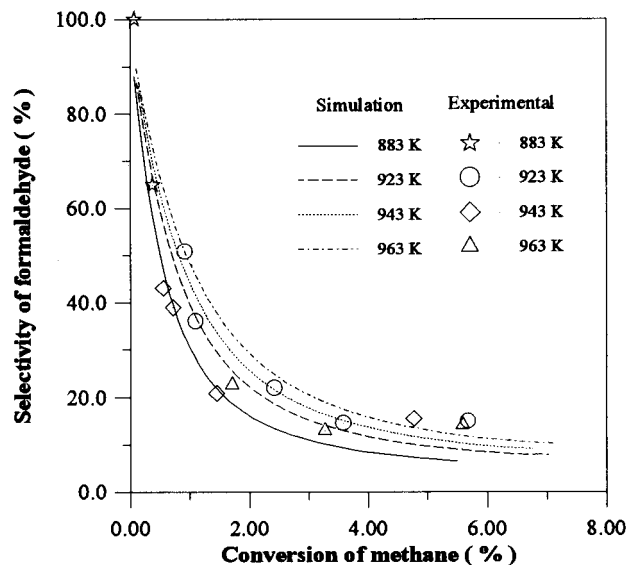


Figure 5. Selectivity to formaldehyde vs methane conversion in a fixed-bed reactor.

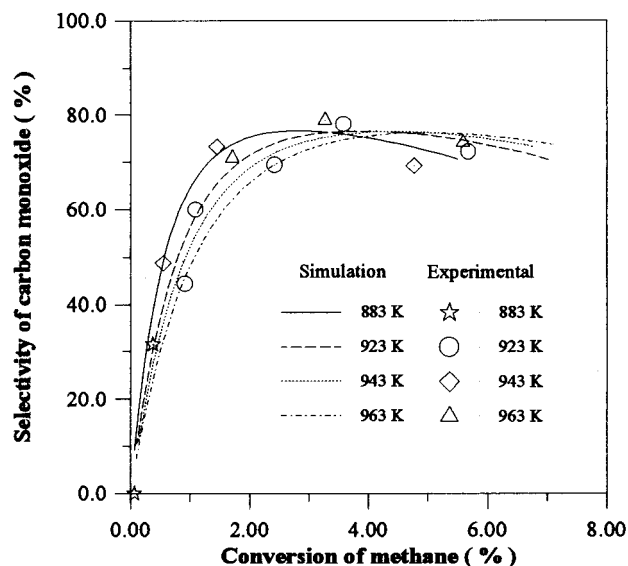
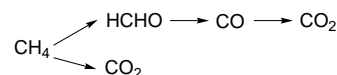


Figure 6. Selectivity to carbon monoxide vs methane conversion in a fixed-bed reactor.

a secondary product that came from further formaldehyde oxidation. Moreover, because the selectivity to carbon dioxide still increased slowly with methane conversion, CO₂ may not only be produced mainly from complete methane oxidation but also from the oxidation of CO. The reaction pathway for the selective oxidation of methane over the Mo-Co-B-O/SiO₂ catalyst may be proposed as the following:



Similar observations of methane partial oxidation over different silica-supported molybdenum oxide catalysts have been reported (Bañares et al., 1994; Faraldos et al., 1996; Spencer et al., 1990; Spencer, 1988). The nature of catalytic activity of cobalt- and boron-doped silica-supported molybdenum oxide catalysts (Mo-Co-B-O/SiO₂) in this work is especially similar to that of a sodium-doped molybdenum oxide catalyst (Spencer et al., 1990).

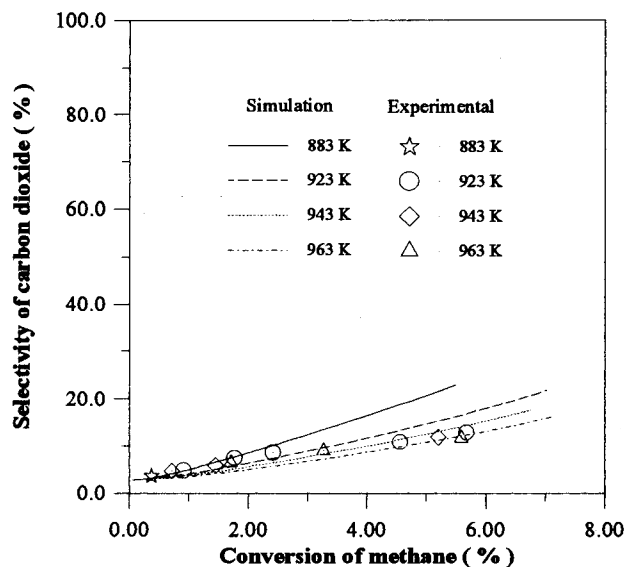
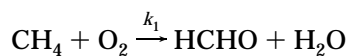
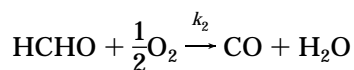


Figure 7. Selectivity to carbon dioxide vs methane conversion in a fixed-bed reactor.

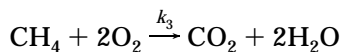
The corresponding stoichiometric equations and rate expressions used for the Mo-Co-B-O/SiO₂ catalyst are as follows:



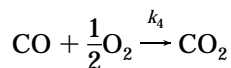
$$\text{RK}_1 = k_1 C_{\text{CH}_4}^{m_1} C_{\text{O}_2}^{n_1}$$



$$\text{RK}_2 = k_2 C_{\text{HCHO}}^{m_2} C_{\text{O}_2}^{n_2}$$



$$\text{RK}_3 = k_3 C_{\text{CH}_4}^{m_3} C_{\text{O}_2}^{n_3}$$



$$\text{RK}_4 = k_4 C_{\text{CO}}^{m_4} C_{\text{O}_2}^{n_4}$$

where the Arrhenius equation is

$$k_i = k_i^0 \exp(-E_i/RT), \quad i = 1-4$$

The Thiele modulus and the internal effectiveness factors were estimated. The values of the estimated Thiele modulus are smaller than 0.2 and the internal effectiveness factors close to 1. The methane oxidation reaction in this work is found to be kinetically controlled. On the basis of the kinetic model for the methane oxidation reaction on the sodium-doped MoO₃/SiO₂ catalyst (Spencer et al., 1990), the kinetic parameters were obtained by minimizing the sum of the relative standard deviations between the measured and calculated conversions and selectivities using an optimization method. The optimized values of the kinetic parameters are reported in Table 1. The relationships of selectivities and methane conversions corresponding to the kinetic model predictions at different temperature

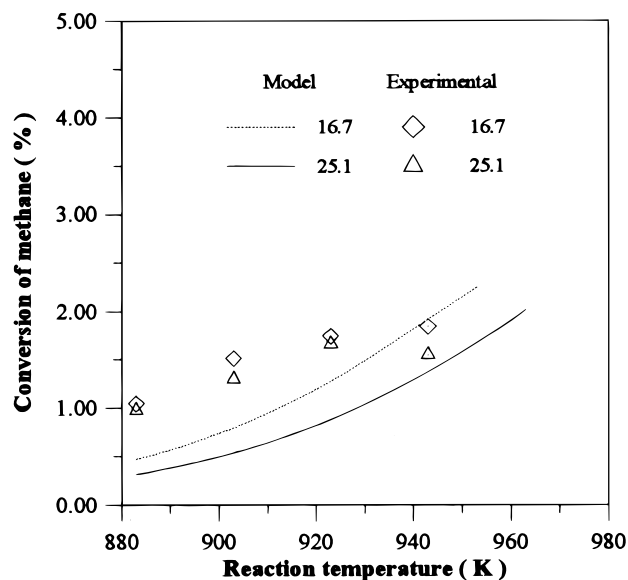


Figure 8. Influence of temperature on methane conversion in a membrane reactor (16.7 or 25.1 L/h is the different feed flow rate of methane.)

Table 1. Kinetic Parameters for Catalytic Oxidation of Methane

<i>i</i>	reaction	k_i^0 (s ⁻¹)	E_i (kJ/mol)	m_i	n_i
1	CH ₄ → HCHO	6.80 × 10 ⁹	189	1.0	0.3
2	HCHO → CO	1.09 × 10 ⁹	134	1.0	0.5
3	CH ₄ → CO ₂	2.30 × 10 ⁸	189	1.0	0.0
4	CO → CO ₂	3.50 × 10 ⁶	117	1.0	0.0

are used to draw the lines in Figures 5–7. The correspondence between kinetic model lines and experimental results is not very good, which would cause a rise in the deviation between the membrane reactor model and experiment.

Membrane Reactor Experimental and Modeling Studies. The membrane reactor experiments were carried out with a methane to oxygen feed ratio of 7.5/1 at atmospheric pressure in a temperature range of 883–943 K. Methane was introduced on the tube side while oxygen flowed concurrently on the shell side. The influences of temperature and methane flow rate on methane conversions are shown in Figures 8 and 9. From these figures, it can be seen that methane conversion increases as the temperature is increased or the methane flow rate is decreased (i.e., reaction residence time increases). The methane conversions and the main oxidation product selectivities obtained at different temperatures are presented in Figures 10–12, respectively.

To find optimum reaction conditions and provide a broad understanding of the membrane reactors for the directions on experimental studies, the mathematical model has been developed to simulate the performance of the packed-bed membrane reactor for partial oxidation of methane to formaldehyde. The parameters used for the simulations are shown in Table 2.

The reaction kinetic rate expressions are adopted from the above-mentioned simulation result of the fixed-bed reactor experiments. Gas permeates through the membrane or catalytic layer by Knudsen diffusion or Fick diffusion at a low pressure and high temperature. The effective diffusion coefficients of all species at different temperatures involved in this reaction system were obtained by experimental measurement and estimation (Shi et al., 1996; Shindo et al., 1983).

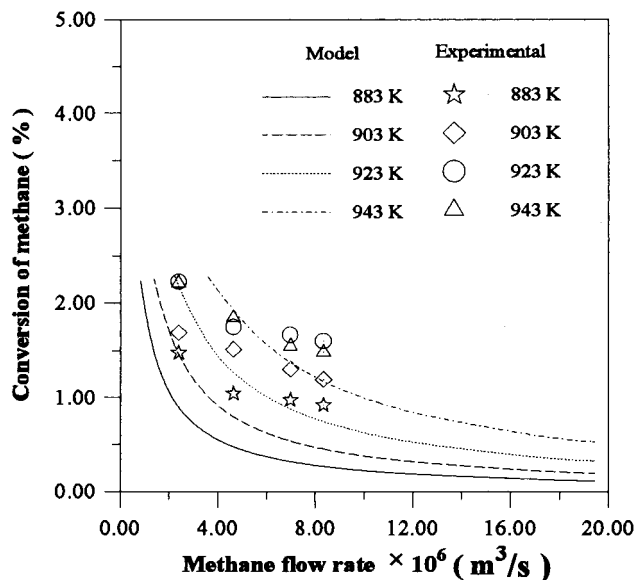


Figure 9. Influence of methane flow rate on methane conversion in a membrane reactor.

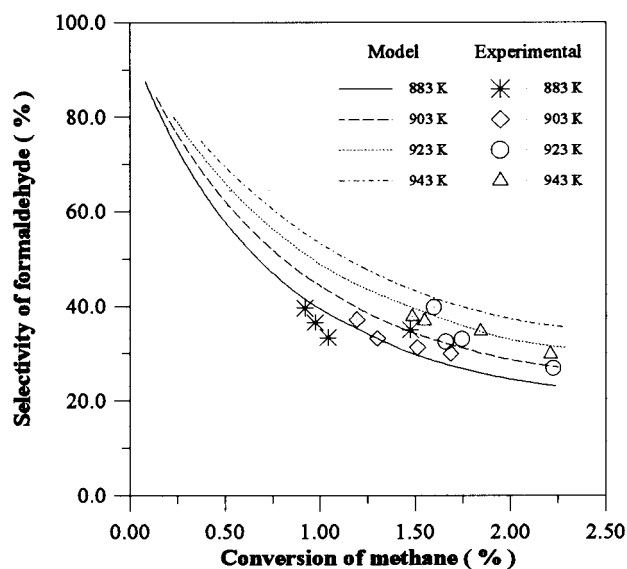


Figure 10. Selectivity to formaldehyde vs methane conversion in a membrane reactor.

Figures 13 and 14 present the dimensionless concentration profiles of methane and formaldehyde in four regions of the membrane reactor at different axial positions calculated by solving the model equations (reaction temperature, 923 K; methane feed flow rate, 20 L/h). The maximum radial gradients for concentration are apparently in the membrane top layer, which implies that the mass transfer is strongly influenced by the membrane resistance. According to the estimation of effective diffusion coefficients, the type of transport mechanism through the membrane top layer at high temperature is Knudsen flow (Saracco and Specchia, 1994). The membrane reactor model is used to fit the experimental data shown in Figures 10–12. The lack of correspondence between model lines and experimental results is brought about by not only the deviation of model parameters (such as kinetic parameters, estimated effective diffusion coefficients) but also the deviation of membrane reactor experiments.

Figure 15 compares the different correlations of the selectivity to formaldehyde and the conversion of meth-

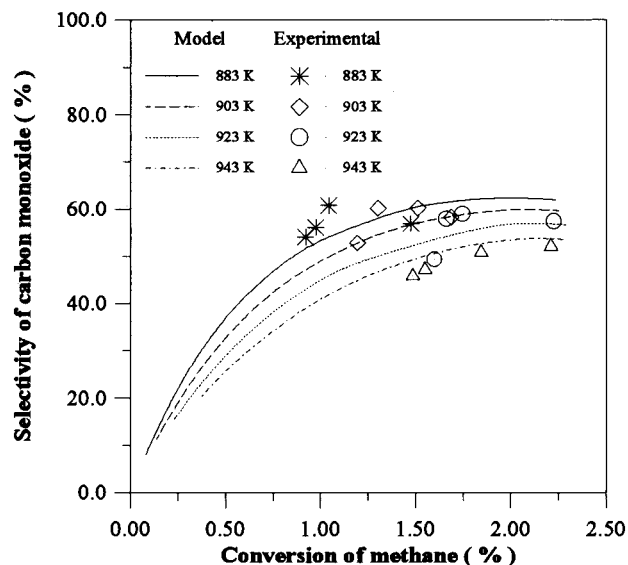


Figure 11. Selectivity to carbon monoxide vs methane conversion in a membrane reactor.

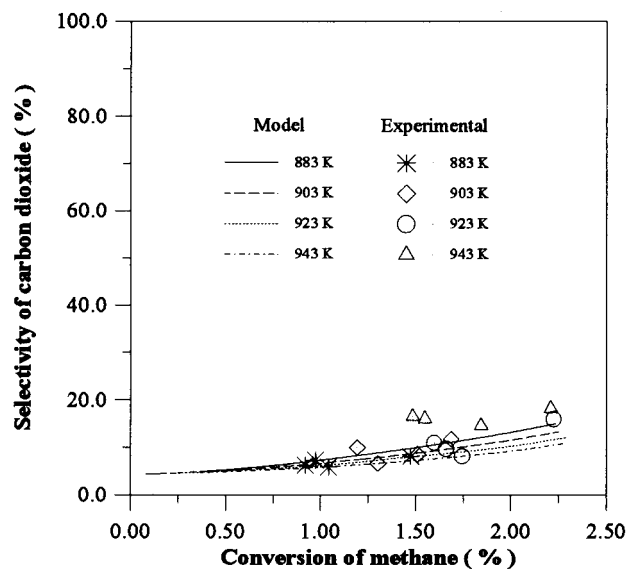


Figure 12. Selectivity to carbon dioxide vs methane conversion in a membrane reactor.

Table 2. Geometry and Properties for the Membrane Reactor

thickness of the zirconia top layer (μm)	20–50
thickness of the α -alumina support layer (mm)	2.5
porosity of the zirconia top layer (%)	40
porosity of the α -alumina support layer (%)	38.5
porosity of the catalytic layer (%)	30
virtual length of the reactor (m)	0.05
inner radius of the membrane tube (mm)	3.5
inner radius of the stainless steel reactor housing (mm)	12.5

ane using the fixed-bed reactor and packed-bed membrane reactor. The membrane reactor gives a considerably better selectivity to the desired product at the same methane conversion; however, the lower methane conversion is obtained. According to the results of simulation and experiments, the enhancement of formaldehyde yield is not very significant when the catalytic reactions are operated under similar conditions (i.e., temperature, pressure, reactant flow rate, geometry of reactor).

To discuss the influence of membrane pore size on the performance of the membrane reactor, the selectivities

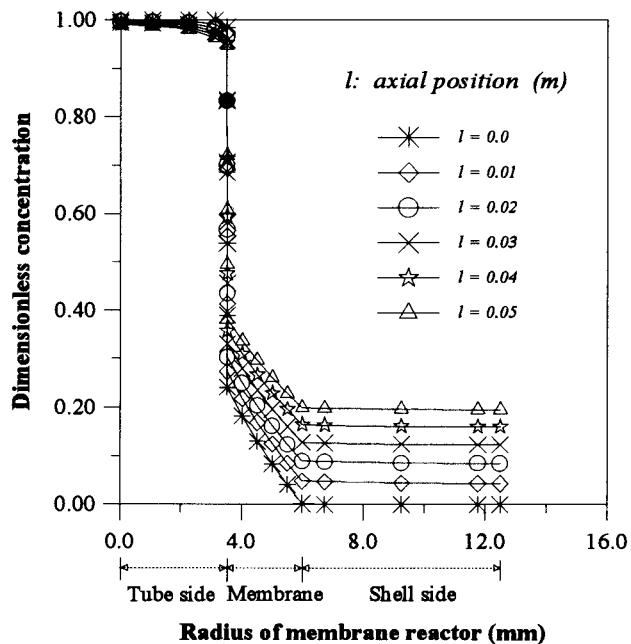


Figure 13. Methane concentration profiles in a membrane reactor.

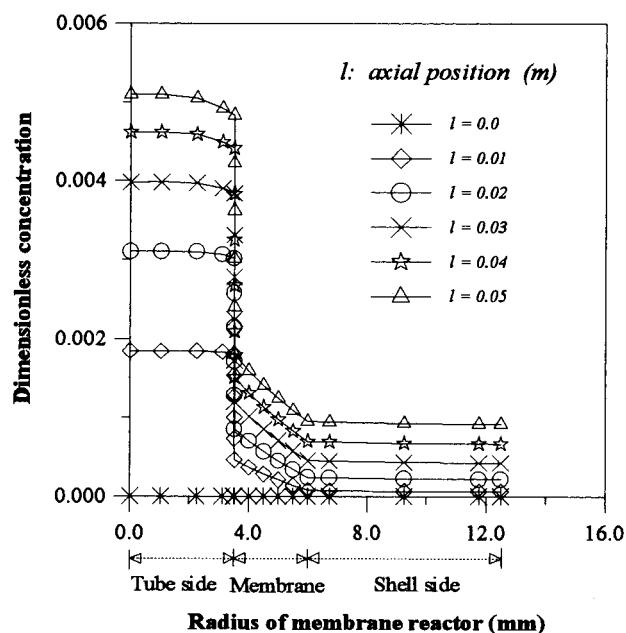


Figure 14. Formaldehyde concentration profiles in a membrane reactor.

to formaldehyde versus methane conversions with membranes of different pore sizes are shown in Figure 16, which is calculated from the packed-bed membrane reactor model. At lower methane conversions the selectivities obtained with different membranes will approximately be the same. Although a higher selectivity is attained with a smaller pore size membrane at a high methane conversion level, no distinct improvement on selectivity has been found. In addition, the simulations indicate that the relationship of methane conversion and the selectivity to formaldehyde will not vary evidently with the porosity or thickness of membrane on the whole.

According to the above results of experiments and simulations, microporous oxide membranes may not be well-suited for the commercial application of membrane reactors for the partial oxidation of methane to form-

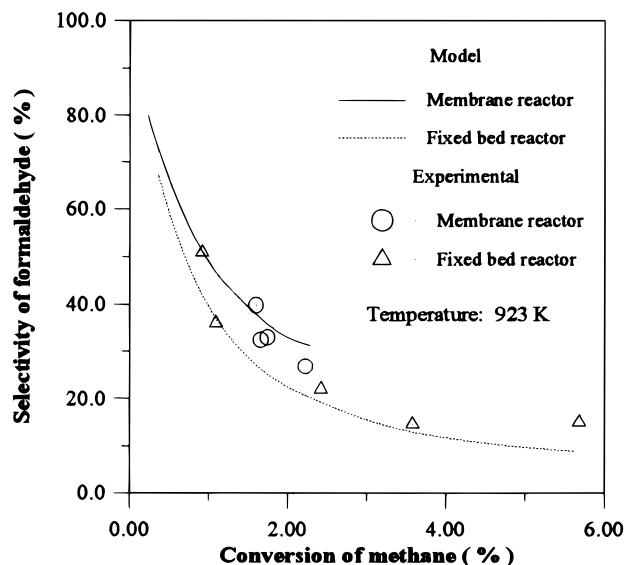


Figure 15. Comparison of the performance between fixed-bed and membrane reactors.

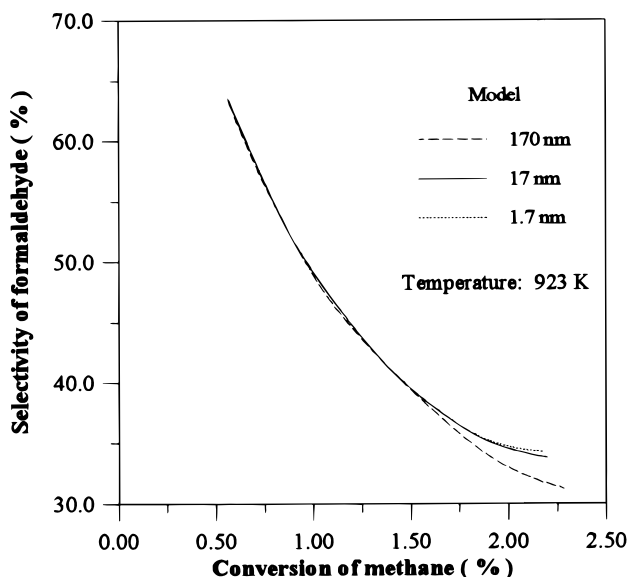


Figure 16. Influence of the pore size of a membrane on the performance of a membrane reactor.

aldehyde over the Mo-Co-B-O/SiO₂ catalyst. This can be qualitatively explained by taking into account the reaction kinetics and membrane permselectivity. For series and series-parallel reactions in a packed-bed plug-flow membrane reactor, the most critical parameters related to the yield of the desired products are the Damköhler-Peclet number product (rate of reaction relative to the rate of membrane permeation) and the ratio of the permeability of the intermediate product to the permeability of the reactant (Bernstein and Lund, 1993). As shown in the reaction kinetic rate expressions, the concentration of methane has a strong effect on the reaction rate, but the effect of oxygen concentration is not strong when the feed mole ratio of methane to oxygen is about 7.5/1. The methane or formaldehyde permeation rate through a microporous membrane is faster than that of oxygen in a Knudsen diffusion regime at low pressure and high temperature; therefore, the membrane reactor cannot allow a more controllable operation and give a distinctly higher yield than the fixed-bed reaction for the conditions investigated.

Several routes may be used to enhance the yield of C_1 oxygenates for partial oxidation of methane. First, new low-cost catalysts with high activity, selectivity, and stability should be developed. Second, the reactor configurations and operation processes should be optimized. Membrane reactors have great potentialities for methane oxidation reactions. It is necessary to develop new membrane materials with high oxygen permeability and selectivity for commercial membrane reactors. If a permselective membrane (such as a dense zirconia membrane permeable only to oxygen) is applied to the catalytic partial oxidation reaction, an improvement in desired product selectivities may be gained. The product formation rates would be very low due to the low oxygen permeabilities of metal membranes (i.e., Ag membranes, etc.) and solid-electrolyte membranes (i.e., dense stabilized zirconia membranes, etc.) (Bhave, 1991; Saracco and Specchia, 1994). Some perovskite membranes (Dixon et al., 1994; Lu et al., 1994; Nozaki and Fujimoto, 1994; Tsai, 1996; Wang and Lin, 1994) have been reported to have oxygen permeation rates 1 or 2 orders of magnitude greater than those of stabilized zirconia membranes. However, higher oxygen permeation rates are generally observed at higher temperature (>700 °C) in these perovskite membranes. Too high temperature is unfavorable for the selectivities to C_1 oxygenates. Recent reports (Balachandran et al., 1995a,b; Tsai, 1996) suggest there is considerable commercial interest in the use of dense perovskite membrane reactors to carry out the methane partial oxidation to syngas reaction that is operated at high temperature (>700 °C generally). Therefore, in the third approach the route via synthesis gas would be more commercially feasible than this direct oxidation method due to the higher yields. Synthesis gas can be further utilized for downstream processes, such as formaldehyde or methanol synthesis. The experimental and modeling studies on dense membrane reactors for partial oxidation of methane will be discussed in detail in the future.

Conclusions

The microporous zirconia/ α -alumina membrane reactor packed with a Mo-Co-B-O/SiO₂ catalyst has been developed for the partial oxidation of methane to formaldehyde in this work. In comparison with the conventional fixed-bed reactor, the membrane reactor could result in a higher selectivity to the desired product. A mathematical model for the packed-bed membrane reactor that fits the experimental data over the range of operation conditions is also presented to simulate the performance of the membrane reactor under different operating conditions. However, no distinct improvement on selectivity to the desired product has been obtained while a microporous oxide membrane is used. A porous membrane may not be well appropriate to the commercial application of membrane reactors for the partial oxidation of methane to formaldehyde. To obtain more significant enhancement of formaldehyde yield, a more permselective and controllable membrane is proposed to replace the microporous oxide membrane.

Acknowledgment

The authors are very grateful for financial support by the National Advanced Materials Committee of China and the Ministry of Chemical Industry of China.

Nomenclature

- C_{ji} = gas concentration of component i in region j (mol/m³)
 C_{ji}^0 = feed concentration of component i in region j (mol/m³)
 \tilde{C}_{ji} = dimensionless concentration of component i in region j
 D_{ji} = effective diffusivity for component i in region j of the membrane reactor (m²/s)
 E_i = apparent activation energy of reaction i (J/mol)
 k_i = reaction rate constant of reaction i (s⁻¹)
 k_i^0 = preexponential factor of reaction i (s⁻¹)
 l = axial distance of the membrane reactor (m)
 \tilde{l} = dimensionless axial distance of the membrane reactor
 L = total length of the reactor (m)
 m_i, n_i = apparent reaction order, $i = 1-4$
 r = radial distance (m)
 \tilde{r} = dimensionless radial distance
 R = universal gas constant (8.314 J/mol·K)
 R_1 = inner radius of the membrane (m)
 R_2 = inner radius of the support layer (m)
 R_3 = outer radius of the membrane (m)
 R_4 = inner radius of the reactor shell (m)
 T = temperature (K)
 u_1 = mean velocity in the tube side (m/s)
 u_4 = mean velocity in the shell side (m/s)

Greek Symbols

- α_{ni} = stoichiometric coefficient of component i for reaction n
 ϵ_1 = external porosity of the catalytic bed

Literature Cited

- Armor, J. N. Catalysis with Permselective Inorganic Membranes. *Appl. Catal.* **1989**, *49*, 1.
 Balachandran, U.; Dusek, J. T.; Sweeney, S. M.; Poepfel, R. B.; Mieville, R. L.; Maiya, P. S.; Kleefisch, M. S.; Pei, S.; Kobylinski, T. P.; Udovich, C. A.; Bose, A. C. Methane to Syngas via Ceramic Membranes. *Am. Ceram. Soc. Bull.* **1995a**, *74*, 71.
 Balachandran, U.; Dusek, J. T.; Mieville, R. L.; Poepfel, R. B.; Kleefisch, M. S.; Pei, S.; Kobylinski, T. P.; Udovich, C. A.; Bose, A. C. Dense Ceramic Membranes for Partial Oxidation of Methane to Syngas. *Appl. Catal.* **1995b**, *133*, 19.
 Bañares, M. A.; Spencer, N. D.; Jones, M. D.; Wachs, I. E. Effect of Alkali Metal Cations on the Structure of Mo(VI)/SiO₂ Catalysts and its Relevance to the Selective Oxidation of Methane and Methanol. *J. Catal.* **1994**, *146*, 204.
 Becker, Y. L.; Dixon, A. G.; Moser, W. R.; Ma, Y. H. Modeling of Ethylbenzene Dehydrogenation in a Catalytic Membrane Reactor. *J. Membr. Sci.* **1993**, *77*, 197.
 Bernstein, L. A.; Lund, C. R. F. Membrane Reactors for Catalytic Series and Series-parallel Reactions. *J. Membr. Sci.* **1993**, *77*, 155.
 Bhave, R. R. *Inorganic Membranes Synthesis, Characteristics and Applications*; Van Nostrand Reinhold: New York, 1991.
 Bindjouli, A. B.; Dehouche, Z.; Bernauer, B.; Lieto, J. Numerical Simulation of Catalytic Inert Membrane Reactor. *Comput. Chem. Eng.* **1994**, *18*, s337.
 Dixon, A. G.; Moser, W. R.; Ma, Y. H. Waste Reduction and Recovery Using O₂ Permeable Membrane Reactors. *Ind. Eng. Chem. Res.* **1994**, *33*, 3015.
 Eng, D.; Stoukides, M. Catalytic and Electrocatalytic Methane Oxidation with Solid Oxide Membranes. *Catal. Rev.-Sci. Eng.* **1991**, *33*, 375.
 Faraldos, M.; Bañares, M. A.; Anderson, J. A.; Hu, H.; Wachs, I. E.; Fierro, J. L. G. Comparison of Silica-supported MoO₃ and V₂O₅ Catalysts in the Selective Partial Oxidation of Methane. *J. Catal.* **1996**, *160*, 214.
 Fox, J. M., III. The Different Catalytic Routes for Methane Valorization: an Assessment of Processes for Liquid Fuels. *Catal. Rev.-Sci. Eng.* **1993**, *35*, 169.
 Hsieh, H. P. *Inorganic Membranes for Separation and Reaction*; Elsevier Science B.V.: Amsterdam, The Netherlands, 1996.

- Huang, P. Preparation, Characterization and Application of Alumina Ceramic Membranes. Ph.D. Dissertation, Nanjing University of Chemical Technology, Nanjing, China, 1996.
- Itoh, N.; Shindo, Y.; Haraya, K.; Hakuta, T. A Membrane Reactor Using Microporous Glass for Shifting Equilibrium of Cyclohexane Dehydrogenation. *J. Chem. Eng. Jpn.* **1988**, *21*, 399.
- Itoh, N.; Shindo, Y.; Haraya, K. Ideal Flow Models for Palladium Membrane Reactors. *J. Chem. Eng. Jpn.* **1990**, *23*, 420.
- Krylov, O. V. Catalytic Reactions of Partial Methane Oxidation. *Catal. Today* **1993**, *18*, 209.
- Lu, Y.; Ramachandra, A.; Ma, Y. H.; Moser, W. R.; Dixon, A. G. Reactor Modeling of the Oxidative Coupling of Methane in Membrane Reactors. *The 3rd International Congress on Inorganic Membranes*, Worcester, MA, 1994; p 657.
- Lu, G.; Shen, S.; Wang, R. Direct Oxidation of Methane to Methanol at Atmospheric Pressure in CMR and RSCMR. *Catal. Today* **1996**, *30*, 41.
- Nozaki, T.; Fujimoto, K. Oxide Ion Transport for Selective Oxidative Coupling of Methane with New Membrane Reactor. *AIChE J.* **1994**, *40*, 870.
- Parmaliana, A.; Arena, F.; Frusteri, F.; Miceli, D.; Sokolovskii, V. On the Nature of Active Sites of Silica Based Oxide Catalysts in the Partial Oxidation of Methane to Formaldehyde. *Catal. Today* **1995**, *24*, 231.
- Pitchai, R.; Klier, K. Partial Oxidation of Methane. *Catal. Rev.—Sci. Eng.* **1986**, *28*, 13.
- Sanchez, J.; Tsotsis, T. T. Current Developments and Future Research in Catalytic Membrane Reactors. In *Fundamentals of Inorganic Membrane Science and Technology*; Burggraaf, A. J., Cot, L., Eds.; Elsevier Science B.V.: Amsterdam, The Netherlands, 1996; p 529.
- Saracco, G.; Specchia, V. Catalytic Inorganic-membrane Reactors: Present Experience and Future Opportunities. *Catal. Rev.—Sci. Eng.* **1994**, *36*, 305.
- Shi, J.; Wang, G. D.; Yu, G. Z.; Chen, M. H. *Chemical Engineering Handbook*; Chemical Industry Press: Beijing, China, 1996.
- Shindo, Y.; Hakuta, T.; Yoshitome, H.; Inoue, H. Gas Diffusion in Microporous Media in Knudsen's Regime. *J. Chem. Eng. Jpn.* **1983**, *16*, 120.
- Shu, J.; Grandjean, B. P. A.; van Neste, A.; Kaliaguine, S. Catalytic Palladium-based Membrane Reactors: A Review. *Can. J. Chem. Eng.* **1991**, *69*, 1036.
- Shu, J.; Grandjean, B. P. A.; Kaliaguine, S. Asymmetric Pd–Ag/SS Catalytic Membranes for CH₄ Steam Reforming. *Appl. Catal. A* **1994**, *119*, 305.
- Sloot, H. J.; Versteeg, G. F.; van Swaaij, W. P. M. A Nonpermselective Membrane Reactor for Chemical Processes Normally Requiring Stoichiometric Feed Rates of Reactants. *Chem. Eng. Sci.* **1990**, *45*, 2415.
- Sloot, H. J.; Smolders, C. A.; van Swaaij, W. P. M.; Versteeg, G. F. High-Temperature Membrane Reactor for Catalytic Gas–solid Reactions. *AIChE J.* **1992**, *38*, 887.
- Spencer, N. D. Partial Oxidation of Methane to Formaldehyde by Means of Molecular Oxygen. *J. Catal.* **1988**, *109*, 187.
- Spencer, N. D.; Pereira, C. J. Partial Oxidation of CH₄ to HCHO over a MoO₃–SiO₂ Catalyst: a Kinetic Study. *AIChE J.* **1987**, *33*, 1808.
- Spencer, N. D.; Pereira, C. J.; Grasselli, R. K. The Effect of Sodium on the MoO₃–SiO₂-catalyzed Partial Oxidation of Methane. *J. Catal.* **1990**, *126*, 546.
- Sun, Y. M.; Khang, S. J. Catalytic Membrane Reactor: Its Performance in Comparison with Other Types of Reactors. *Ind. Eng. Chem. Res.* **1990**, *29*, 232.
- Torres, M.; Sanchez, J.; Dalmon, J. A.; Bernauer, B.; Lieto, J. Modeling and Simulation of a Three-phase Membrane Reactor for Nitrobenzene Hydrogenation. *Ind. Eng. Chem. Res.* **1994**, *33*, 2421.
- Tsai, C. Y. Perovskite Dense Membrane Reactors for the Partial Oxidation of Methane to Synthesis Gas. Ph.D. Dissertation, Worcester Polytechnic Institute, Worcester, MA, 1996.
- Wang, W.; Lin, Y. S. A Theoretical Analysis of Oxidative Coupling of CH₄ in a Tubular Dense Membrane Reactor. *The 3rd International Congress on Inorganic Membranes*, Worcester, MA, 1994; p 259.

Received for review December 9, 1997

Revised manuscript received April 16, 1998

Accepted April 22, 1998

IE970893C